Augmented saddle point formulation of the steady-state Stefan–Maxwell diffusion problem

ALEXANDER VAN-BRUNT †,

Mathematical Institute, University of Oxford, Oxford, OX2 6GG, UK and
The Faraday Institution, Harwell Campus, Didcot, OX11 ORA, UK
PATRICK E. FARRELL ‡
Mathematical Institute, University of Oxford, Oxford, OX2 6GG, UK
AND
CHARLES W. MONROE §
Department of Engineering Science, University of Oxford, Oxford OX1 3PJ, UK and
The Faraday Institution, Harwell Campus, Didcot, OX11 ORA, UK

[Received on 5 June 2020]

We investigate structure-preserving finite element discretizations of the steady-state Stefan–Maxwell diffusion problem which governs diffusion within a phase consisting of multiple species. An approach inspired by augmented Lagrangian methods allows us to construct a symmetric positive definite augmented Onsager transport matrix, which in turn leads to an effective numerical algorithm. We prove inf-sup conditions for the continuous and discrete linearized systems and obtain error estimates for a phase consisting of an arbitrary number of species. The discretization preserves the thermodynamically fundamental Gibbs–Duhem equation to machine precision independent of mesh size. The results are illustrated with numerical examples, including an application to modelling the diffusion of oxygen, carbon dioxide, water vapour and nitrogen in the lungs.

Keywords: Stefan–Maxwell equations, multicomponent diffusion, augmented saddle point formulation

1. Introduction

Molecular diffusion is a fundamental mode of mass transport. Within a stationary solution containing a dilute solute species of concentration c, the classical model for diffusion was formulated by Fick (1855), which postulates that the solute's molar flux N obeys

$$N = -D\nabla c, \tag{1.1}$$

in which $D > 0$ is the solute's Fickian diffusivity in the solution. Maxwell (1867) applied kinetic theory to derive Fick's law for binary ideal-gas diffusion, showing for isothermal gases that D further relates to a composition-independent constant material property. Stefan (1871) extended Maxwell's analysis to multicomponent gases, expressing the gradient of each species concentration in terms of a matrix of binary diffusivities. The resulting Stefan–Maxwell equations (also commonly called Maxwell–Stefan

†Corresponding author. Email: alexander.van-brunt@maths.ox.ac.uk
‡Email: patrick.farrell@maths.ox.ac.uk
§Email: charles.monroe@eng.ox.ac.uk

equations in the engineering and mathematical literature) have been verified experimentally for gas diffusion in studies such as Duncan & Toor (1962) and Carty & Schrodt (1975).

Using his theory of irreversible thermodynamics, Onsager (1931a,b, 1945) provided a broader theoretical framework for mass transport that could also be applied to multicomponent diffusion in nonideal phases, including liquids and/or solids. Hirschfelder *et al.* (1954) substantiated this more abstract analysis, manipulating thermodynamic laws and hydrodynamic equations to construct the diffusion driving forces for general nonisobaric, nonisothermal, multicomponent diffusion systems. Combined with Lightfoot, Cussler and Rettig's observation that the Stefan–Maxwell diffusivities map invertibly into Onsager's transport matrix, and can therefore be used for condensed phases as well as gases (Lightfoot *et al.*, 1962), this extended the Stefan–Maxwell theory to all molecular diffusion processes. Newman *et al.* (1965) brought the generalization further, accounting for materials containing charged solutes, thereby completing the development of the contemporary Stefan–Maxwell equations. Modern expositions of the theory can be found in Krishna & Wesselingh (1997); Standart *et al.* (1979) and Datta & Vilekar (2010).

Given a bounded Lipschitz domain $\Omega \subset \mathbb{R}^d$, $d \in \{2,3\}$, the Stefan–Maxwell equations describing the diffusion of the n species that constitute a common phase at a given absolute temperature $T > 0$ are given by

$$d_i = \sum_{\substack{j=1 \\ i \neq j}}^{n} \frac{RTc_i c_j}{\mathscr{D}_{ij} c_{\mathrm{T}}} (v_i - v_j) \tag{1.2}$$

for $i = 1,2,\ldots,n$, in which $R > 0$ is the ideal gas constant. The terms $c_i : \Omega \to \mathbb{R}^+$ and $v_i : \Omega \to \mathbb{R}^d$ denote the concentration and velocity of species $i = 1,2,\ldots,n$ respectively, related to the molar flux of the i^{th} species by $N_i = c_i v_i$. For species $i \neq j$, $\mathscr{D}_{ij} \in \mathbb{R}$ represents the Stefan–Maxwell diffusivity of species i through species j; these material parameters are symmetric in the species indices, $\mathscr{D}_{ij} = \mathscr{D}_{ji}$, and coefficients $\mathscr{D}_{ii}$ are not defined. The term c_{T} in equation (1.2) denotes the total concentration, defined as

$$c_{\mathrm{T}} := \sum_{i=1}^{n} c_i, \tag{1.3}$$

and the terms $d_i : \Omega \to \mathbb{R}^d$ represent the diffusion driving forces, which generally depend on the species concentrations, temperature and pressure. In the case of isothermal, isobaric ideal-gas diffusion considered here, $d_i = -RT\nabla c_i$. Furthermore, an ideal gas satisfies the equation of state

$$p = c_{\mathrm{T}} RT, \tag{1.4}$$

in which p is the pressure. Hence in the isothermal, isobaric setting, c_{T} is a constant. To pose the Stefan–Maxwell convection-diffusion problem, flux constitutive laws (1.2) and the equation of state (1.4) are coupled to the continuity equations

$$\frac{\partial c_i}{\partial t} = -\nabla \cdot \big(c_i v_i\big) + r_i, \tag{1.5}$$

where $r_i : \Omega \to \mathbb{R}$ is a specified volumetric reaction rate, which quantifies the generation or depletion of species i by homogeneous chemical reactions. Under the ideal-gas assumption considered in this paper, we are interested in solving (1.2) (with $d_i = -RT\nabla c_i$) and (1.5) for the species concentrations c_i and their respective velocities v_i.

The Stefan–Maxwell equations have found a diverse range of applications in areas such as biology, electrochemistry, and plasma physics. For specific examples, we refer the reader to the studies by

Boudin *et al.* (2010); Robertson & Zydney (1988); Abdullah & Das (2007); Newman & Thomas-Alyea (2012); Liu & Monroe (2014) and Kolesnikov & Tirskii (1984). Because they account for solute/solute interactions as well as solute/solvent interactions, Stefan–Maxwell models can exhibit fundamentally different behaviour from Fickian models. For example, in Duncan & Toor (1962) 'uphill diffusion' is observed, wherein the directions of a species' molar flux and its concentration gradient coincide, in contradiction to (1.1). In electrochemistry, the Stefan–Maxwell formalism justifies surprising observations like negative transference, where the flow of an electric current with one sign carries ions of opposing sign along with it (Monroe & Delacourt, 2013).

Under restrictive assumptions, a multicomponent extension of Fick's law known as *dilute solution theory* can be recovered. For a dilute set of species c_k, $k = 2, \dots, n$ in the presence of a solvent in far greater proportions, c_1, one can formally neglect the terms $c_i c_j$ in (1.2) whenever both $i, j \geqslant 2$ and take $c_{\mathrm{T}} \approx c_1$, allowing rearrangement to express the molar fluxes as

$$N_i = \frac{\mathscr{D}_{i1}}{RT} d_i + c_i v_1. \tag{1.6}$$

For dilute solutes the driving forces often take the form $d_i = -\chi_i RT \nabla c_i$, where χ_i is known as a Darken factor (Darken, 1948), in which case one can identify $D_i = \mathscr{D}_{i1}\chi_i$ as the Fickian diffusivity of species i in the solution. Writing equations (1.6) for all solutes and replacing v_1 with the barycentric velocity v produces the dilute solution theory. We direct the reader to Newman & Thomas-Alyea (2012) for further details. When the solute driving forces within dilute solution theory are written in terms of both concentration gradients and the electric field, (1.6) is referred to as a Nernst–Planck relationship, based on the work by Nernst (1888) and Planck (1890). Nernst–Planck equations have been extensively studied in the mathematical literature, sometimes coupled with Poisson's equation to account for the distribution of the electric potential, and a Navier–Stokes equation or a Darcy flow to compute the velocity v. We refer the reader to Schmuck (2009); Herz *et al.* (2012); Liu *et al.* (2015) and Bousquet *et al.* (2018) and the references therein for the existing mathematical literature on the Nernst–Planck equation. In many cases dilute solution theory is not appropriate, and the full Stefan–Maxwell equations must be considered. A comparison of Fickian to Stefan–Maxwell diffusion profiles for gases can be found in Krishna & Wesselingh (1997) and Boudin *et al.* (2010). Examples of the limitations of dilute-solution models are discussed in the context of lung modelling, earth science and electrolyte transport in the studies by Chang *et al.* (1975); Baehr & Bruell (1990) and Bizeray *et al.* (2016) respectively.

1.1 *Physical structure and consequences*

The mathematical structure of irreversible thermodynamics will prove useful below for devising discretizations and error estimates for the Stefan–Maxwell diffusion problem. We therefore summarize some key points of the theory. We begin with the transport equations postulated by Onsager (1945) for isotropic materials,

$$d_i = \sum_{j=1}^{n} \mathbf{M}_{ij} v_j, \tag{1.7}$$

in which the statistical reciprocal relations developed in Onsager (1931a,b) require the transport matrix $\mathbf{M} : \Omega \to \mathbb{R}^{n\times n}$ to be real symmetric.

The Onsager transport equations (1.7) were developed independently of the Stefan–Maxwell theory (1.2). It was subsequently realized by Lightfoot *et al.* (1962) that the Stefan–Maxwell equations could

be understood in terms of Onsager's transport matrix by identifying

$$\mathbf{M}_{ij} = \mathbf{M}_{ij}(c_i, c_j, c_\mathrm{T}) = \begin{cases} -\frac{RTc_ic_j}{\mathscr{D}_{ij}c_\mathrm{T}} & \text{if } i \neq j \\ \sum_{k\neq i}^{n} \frac{RTc_ic_k}{\mathscr{D}_{ik}c_\mathrm{T}} & \text{if } i = j \end{cases} \tag{1.8}$$

as the entries of $\mathbf{M}$.

Time evolution of nonequilibrium states leads to local entropy production, denoted by $\dot{S}$. For an isothermal, isobaric system with a given collection of species velocities $(v_1, v_2, \ldots, v_n)$ experiencing $(d_1, d_2, \ldots, d_n)$ nonequilibrium diffusion driving forces, the balances of material, momentum, and heat are manipulated in Hirschfelder *et al.* (1954) and Monroe & Newman (2009) to write the entropy production of isothermal diffusion as

$$\dot{S} = \frac{1}{T}\sum_{i=1}^{n} d_i \cdot v_i, \tag{1.9}$$

in which the d_i are identified as functions of the gradients of temperature, pressure, and $(c_1, c_2, ..., c_n)$ by grouping terms in the Gibbs–Duhem equation from equilibrium thermodynamics (de Groot & Mazur, 1962; Hirschfelder *et al.*, 1954; Goyal & Monroe, 2017). In general there may be other terms in (1.9) such as viscous dissipation or reaction entropy, but these will be neglected here.

The second law of thermodynamics further demands that the energy dissipation $T\dot{S}$ is non-negative, $T\dot{S} \geqslant 0$, with equality only in an equilibrium state, which is defined by the condition that $d_i = 0$ for all i. Thermodynamic stability therefore requires further that $\mathbf{M}$ be positive semidefinite.

Some additional structure of the transport matrix is specific to multicomponent mass diffusion. Importantly, the theory must guarantee that diffusional motion, driven by thermodynamic property gradients, remains distinct from species convection, a non-dissipative process driven by bulk flow. This distinction is made by requiring that (1.7) be invariant to a shift of every species velocity by a vector field $\bar{v} : \Omega \to \mathbb{R}^d$, i.e. the equation remains unchanged when each v_i in (1.7) is replaced by $(v_i - \bar{v})$. The essential physical distinction between diffusion and convection consequently requires that

$$\sum_{j=1}^{n} \mathbf{M}_{ij} = 0, \tag{1.10}$$

as noted by Onsager (1945) and Helfand (1960). Hence $\mathbf{M}$ has a null eigenvalue corresponding to the eigenvector $(1, 1, \ldots, 1)^\top \in \mathbb{R}^n$. Invariance with respect to the convective velocity is naturally embedded in the Stefan–Maxwell form (1.2), because $v_i - v_j = (v_i - \bar{v}) - (v_j - \bar{v})$.

The symmetry of $\mathbf{M}$ suggested by Onsager (1945) requires that $\mathscr{D}_{ij} = \mathscr{D}_{ji}$, a fact that has also been demonstrated directly for Stefan–Maxwell diffusion by fluctuation theory in Monroe *et al.* (2015). The symmetry of the transport matrix combined with the nullspace (1.10) allows recovery of the full Gibbs–Duhem equation, namely

$$\sum_{i=1}^{n} d_i = 0. \tag{1.11}$$

In the context of transport theory, equation (1.11) can be seen as a statement of Newton's third law of motion, that action equals reaction. In thermodynamics this is necessary to be consistent with the first law of thermodynamics and the extensivity of the Gibbs free energy.

Reasoning physically that all diffusion processes are necessarily dissipative, Onsager (1945) makes the stronger assumption that $\mathbf{M}$ has exactly one null eigenvalue. Taken together, the physical arguments

require that $\mathbf{M}$ is symmetric positive semidefinite, and that its eigenvalues, $\{\lambda_{i=1}^{\mathbf{M}}\}_{i=1}^{n}$, may be ordered as

$$0 = \lambda_1^{\mathbf{M}} < \lambda_2^{\mathbf{M}} \leqslant \cdots \leqslant \lambda_n^{\mathbf{M}}, \tag{1.12}$$

a spectral structure that will be used throughout this paper.

Combining (1.7) and (1.9) implies that

$$T\dot{S} = \sum_{i,j=1}^{n} v_i \cdot \mathbf{M}_{ij} v_j = \frac{1}{2} \sum_{i=1}^{n} \sum_{j \neq i}^{n} \frac{c_i c_j RT}{\mathscr{D}_{ij} c_{\mathrm{T}}} (v_j - v_i)^2 \geqslant 0. \tag{1.13}$$

At positive concentrations, energy dissipation $T\dot{S} > 0$ occurs whenever there is relative species motion, implying that the equality in (1.13) occurs if and only if $v_1 = v_2 = \cdots = v_n$.

One must take care to note that $\mathbf{M}$ may afford additional nullspaces beyond (1.10) if any concentration vanishes. Consequently, in order to phrase the Stefan–Maxwell equations in terms of Onsager's transport laws (1.7) with a transport matrix $\mathbf{M}$ that possesses the spectral structure (1.12), it will be necessary to assume that $c_i > 0$ almost everywhere for each $i = 1, 2, \ldots n$. We make this assumption henceforth.

Because the present discussion is limited to ideal-gas mixtures, it can be assumed that the Stefan–Maxwell diffusion coefficients $\mathscr{D}_{ij}$ are given constants, which places even stronger restrictions on their values. Whenever the concentrations satisfy $c_i \geqslant \kappa > 0$ for each $i = 1, 2, \ldots, n$ and any positive constant κ, then $\lambda_\kappa \leqslant \lambda_2^{\mathbf{M}}$ for a positive constant λ_κ which depends only on κ, a fact that will be used throughout the paper. From the calculation (1.13), it follows that a necessary and sufficient condition for (1.12) to be true for all positive concentrations is that each $\mathscr{D}_{ij}$ is strictly positive (Standart *et al.*, 1979). It must be stressed, however, that the Stefan–Maxwell diffusion coefficients in many physical systems depend strongly on the concentrations of the species, in which case negative Stefan–Maxwell diffusion coefficients are not only possible, but are observed and of practical interest (Kraaijeveld & Wesselingh, 1993; Villaluenga *et al.*, 2018). Therefore in order to present a general framework for multispecies diffusion, the results in this paper only use the spectral structure (1.12), not the positivity of the Stefan–Maxwell diffusion coefficients.

In systems with more than one spatial dimension, the existence of the nullspace (1.10) means that the problem (1.2), (1.3), (1.5) will not be well-posed unless a choice of convective velocity is made (see Remark 3.1 below for the one-dimensional case). This can be done by specifying that the mass-flux must equal given data $u : \Omega \to \mathbb{R}^d$:

$$u = \sum_{j=1}^{n} M_j c_j v_j, \tag{1.14}$$

where $M_i > 0$ is the molar mass of species i. In general, the mass-flux must also be solved for via the Cauchy momentum equation, which in the absence of a pressure gradient or an external force field, can be written in conservation form as

$$\frac{\partial u}{\partial t} = -\nabla \cdot \Big(\rho^{-1} u \otimes u - \sigma \Big), \tag{1.15}$$

where the density ρ is defined as

$$\rho := \sum_{j=1}^{n} M_j c_j, \tag{1.16}$$

and σ denotes the deformation stress tensor appropriate for the medium. We refer to the problem of solving (1.2), (1.5), (1.14) and (1.15) as the Stefan–Maxwell convection-diffusion problem. In this

work we assume that u is given and focus on the solution of (1.2), (1.5) and (1.14) under an additional steady-state assumption, which we call the steady-state Stefan–Maxwell diffusion problem.

1.2 *Premise and main results*

The central idea of this manuscript is to incorporate the constraint (1.14) by augmenting (1.2), in a manner inspired by the augmented Lagrangian approach (Bochev & Lehoucq, 2006; Fortin & Glowinski, 1983). Given $\gamma > 0$, for each i we multiply both sides of (1.14) by $\gamma RTM_i c_i/\rho$ and add the resulting term to the i^{th} equation of (1.2) to deduce that

$$d_i + \frac{\gamma RTM_i c_i}{\rho} u = \sum_{j\neq i}^{n} \frac{RTc_i c_j}{\mathscr{D}_{ij} c_{\mathrm{T}}} \big(v_i - v_j\big) + \frac{\gamma RTM_i c_i}{\rho} \sum_{j=1}^{n} M_j c_j v_j = \sum_{j=1}^{n} \mathbf{M}_{ij}^{\gamma} v_j \tag{1.17}$$

for $i = 1, 2, \ldots, n$, where $\mathbf{M}_{ij}^{\gamma}$ is the augmented transport matrix

$$\mathbf{M}_{ij}^{\gamma} = \mathbf{M}_{ij} + \gamma \mathscr{L}_{ij}, \tag{1.18}$$

in which

$$\mathscr{L}_{ij} := RTM_i M_j c_i c_j/\rho. \tag{1.19}$$

Our particular choice of the entries of $\mathscr{L}$ allows us to compute

$$\sum_{i,j=1}^{n} v_i \cdot \mathbf{M}_{ij}^{\gamma} v_j, = \frac{1}{2} \sum_{i=1}^{n} \sum_{j\neq i}^{n} \frac{c_i c_j RT}{\mathscr{D}_{ij} c_{\mathrm{T}}} (v_j - v_i)^2 + \gamma \Big(\sum_{j=1}^{n} M_j c_j v_j \Big)^2 \tag{1.20}$$

to show that the augmented transport matrix is symmetric positive definite. The positive-definiteness achieved by this augmentation will cause the associated bilinear forms in the variational formulation to follow to be coercive, greatly facilitating the analysis.

The paper is organized as follows. Section 2 provides an overview of the existing numerical literature on the Stefan–Maxwell equations and contrasts our approach with previous efforts. In section 3 we derive a suitable weak formulation for the problem and prove well-posedness of a linearized system of (1.2)-(1.5) in section 4. In section 5 we show stability of a discretization of this linearized system and prove error estimates for the linearization. Finally, in section 6 we verify our error estimates with a manufactured solution and illustrate our method by simulating the interdiffusion of oxygen, carbon dioxide, water vapour and nitrogen in the lungs.

2. Existing numerical literature

Despite their wide applicability, the Stefan–Maxwell equations have received relatively little attention from numerical analysts. In nearly all existing work, the equations are formulated in terms of the molar flux $N_i = c_i v_i$. The interdependence among the collection of driving forces implied by Gibbs–Duhem relation (1.11) allows the equation for d_n to be discarded. The mass-flux constraint (1.14) is then used to eliminate the n^{th} species velocity from the system. Following this process, a non-singular matrix $\mathbf{A}$ is derived which satisfies

$$d_i = \sum_{j=1}^{n-1} \mathbf{A}_{ij} c_j v_j = \sum_{j=1}^{n-1} \mathbf{A}_{ij} N_j. \tag{2.1}$$

One can then proceed to solve for the molar fluxes in terms of the driving forces d_i by inverting $\mathbf{A}$. If, for example, we have $d_i = -RT\nabla c_i$, the inverted, truncated flux laws can be substituted into the continuity equations (1.5) for species $i = 1, ..., n-1$ to yield

$$\frac{\partial c_i}{\partial t} = -\nabla \cdot \Big(\sum_{j=1}^{n-1} \mathbf{A}_{ij}^{-1} \nabla c_j \Big). \tag{2.2}$$

Thus one obtains evolution equations for the concentrations, having eliminated the molar fluxes completely. Papers which take this approach and analyse the resulting equations to determine some existence and uniqueness properties include Boudin *et al.* (2012); Bothe (2010); Jüngel & Stelzer (2012) and Jüngel & Leingang (2019). Boudin *et al.* (2012) and Jüngel & Leingang (2019) also analyse numerical schemes along these lines. It is worth remarking that the matrix $\mathbf{A}^{-1}$ is not positive symmetric definite, although, at least in certain circumstances, one can define 'entropy variables' so that the resulting system is symmetric positive definite, as carried out by Jüngel & Leingang (2019).

The approach of McLeod & Bourgault (2014) does not eliminate molar fluxes, but rather solves for them in a mixed saddle point formulation. They then prove well-posedness of a linearized system consisting of three species, under some constraints on the Stefan–Maxwell diffusion coefficients. A discretization using mixed finite elements is then presented and error bounds on the linearized system are obtained. Our paper is similar in scope, but with several key differences and extensions.

First, our approach does not need any rearrangement of (1.14) to eliminate one species, but rather incorporates the constraint via the augmented formulation (1.17). The choice of species to eliminate is somewhat arbitrary, and with the augmentation is no longer necessary. Augmentation also exploits the symmetric positive semidefinite structure of the transport matrix and preserves permutational symmetry of the system. This will be particularly pertinent for anticipated future work where we intend to have more complex driving forces of the form

$$d_i = -c_i \nabla \mu_i + \frac{c_i M_i}{\rho} \nabla p, \tag{2.3}$$

where μ_i is the electrochemical potential of species i and p is the pressure. These more complex driving forces render rearrangement increasingly intractable.

Second, the symmetric positive definite structure of the augmented transport matrix yields straightforward proofs of the coercivity of bilinear forms on appropriate function spaces. As a consequence, we will prove that the linearized system is well-posed in the continuous and discrete setting and derive error bounds for its discretization in the general case of n species. The methodology presented in this paper also encompasses the case where individual Stefan–Maxwell diffusion coefficients may be negative.

Finally, we are able to design the discrete formulation in a structure-preserving way so that the Gibbs–Duhem equation (1.11) is satisfied up to machine precision, independent of mesh size. Previous works instead assume the Gibbs–Duhem equation and use it to infer the concentration of the n^{th} species in a postprocessing step.

3. Problem formulation

We proceed to cast the problem into variational form. Note that both sides of equation (1.17) are proportional to RT and hence without loss of generality we assume that $RT = 1$. Our idealized assumption on the driving forces then becomes

$$d_i := -\nabla c_i, \quad i = 1, 2, \dots n. \tag{3.1}$$

In this case the Gibbs–Duhem equation (1.11) reduces to

$$\nabla c_{\mathrm{T}} = 0, \tag{3.2}$$

i.e. that total concentration is constant. This is also important as the constancy of c_{T} is required to be consistent with the equation of state (1.4), which is distinct from the Gibbs–Duhem equation. We assume that $u \in H^1(\Omega)^d$ and consider the boundary conditions

$$N_i \cdot \mathbf{n} = c_i v_i \cdot \mathbf{n} = g_i \in H^{-1/2}(\Gamma_N) \text{ on } \Gamma_N, \quad i = 1,2,\ldots,n, \tag{3.3}$$

$$c_i = f_i > 0 \in H^{1/2}(\Gamma_D) \text{ on } \Gamma_D, \quad i = 1,2,\ldots,n, \tag{3.4}$$

where $\mathbf{n}$ is the outward facing unit normal vector and Γ_N, Γ_D partition $\partial\Omega$. The equalities in (3.3)-(3.4) are to be understood in the sense of traces (Evans, 2010). It is necessary to assume that f_i is positive for each $i = 1,2,\ldots,n$ to avoid $\mathbf{M}$ acquiring another nullspace at the boundary. Either one of Γ_N and Γ_D may be empty. This boundary data is assumed to satisfy

$$\sum_{i=1}^{n} g_i M_i = u \cdot \mathbf{n} \text{ on } \Gamma_N, \tag{3.5}$$

$$\sum_{i=1}^{n} f_i = C_{\mathrm{T}} \text{ on } \Gamma_D, \tag{3.6}$$

where $C_{\mathrm{T}} > 0$ is a constant that we will show is equal to the total concentration (1.3). These assumptions are necessary to be consistent with the Gibbs–Duhem equation (1.11) and the mass-flux constraint (1.14). Under the steady-state assumption, the species continuity equations (1.5) become

$$\nabla \cdot (c_i v_i) = r_i. \tag{3.7}$$

Therefore, we demand that the reaction rates, $r_i \in L^2(\Omega)$, satisfy

$$\sum_{i=1}^{n} r_i M_i = \nabla \cdot u \text{ in } \Omega \tag{3.8}$$

to ensure consistency of (3.7) with (1.14).

We define the function space

$$H^1_{\Gamma_D}(\Omega) = \{w_i \in H^1(\Omega) : w_i|_{\Gamma_D} = 0\}, \tag{3.9}$$

and the affine function space

$$H^1_{f_i}(\Omega) = \{w_i \in H^1(\Omega) : w_i|_{\Gamma_D} = f_i\}. \tag{3.10}$$

We can now derive the weak formulation. We test (1.17) with $\tau_i \in L^2(\Omega)^d$ and integrate over Ω to derive for all $i = 1,2,\ldots,n$,

$$\int_\Omega \Big(-\nabla c_i + \frac{\gamma M_i c_i}{\rho} u \Big) \cdot \tau_i = \int_\Omega \Big(\sum_{j \neq i}^{n} \frac{c_i c_j}{\mathscr{D}_{ij} c_{\mathrm{T}}} (v_i - v_j) + \frac{\gamma M_i c_i}{\rho} \sum_{j=1}^{n} M_j c_j v_j \Big) \cdot \tau_i, \tag{3.11}$$

for all $\tau_i \in L^2(\Omega)^d$.

For a given $w_i \in H^1_{\Gamma_D}(\Omega)$ we multiply both sides of (3.7) by $-w_i$ and integrate by parts to yield that for all $i = 1,2,\ldots,n$,

$$\int_\Omega c_i v_i \cdot \nabla w_i - \int_{\Gamma_N} g_i w_i = -\int_\Omega r_i w_i, \tag{3.12}$$

for all $w_i \in H^1_{\Gamma_D}(\Omega)$. We therefore seek $v_i \in L^2(\Omega)^d$ and $c_i \in H^1_{f_i}(\Omega)$ such that (3.11) and (3.12) hold for every $\tau_i \in L^2(Q)^d$ and $w_i \in H^1_{\Gamma_D}(\Omega)$, for each $i = 1,2,\ldots,n$.

REMARK 3.1 In the case of one dimension, (3.7) and the boundary data (3.3)-(3.4) allow us to recover $c_i v_i$ completely. Consequently no augmentation is necessary.

We will now show that such a weak solution satisfies both the Gibbs–Duhem equation (1.11) and the mass-flux constraint (1.14). Choosing $\tau_i = \tau \in L^2(\Omega)^d$ for every $i = 1,2,\ldots,n$ and summing over i in (3.11) yields

$$\sum_{i=1}^n \int_\Omega \Big(-\nabla c_i + \frac{\gamma M_i c_i}{\rho} u \Big) \cdot \tau = \sum_{i=1}^n \int_\Omega \Big(\sum_{j\neq i}^n \frac{c_i c_j}{\mathscr{D}_{ij} c_{\mathrm{T}}} (v_i - v_j) + \frac{\gamma M_i c_i}{\rho} \sum_{j=1}^n M_j c_j v_j \Big) \cdot \tau. \tag{3.13}$$

However we can use the nullspace (1.10) and symmetry of $\mathbf{M}$ to deduce

$$\sum_{i=1}^n \sum_{j\neq i}^n \frac{c_i c_j}{\mathscr{D}_{ij} c_{\mathrm{T}}} (v_i - v_j) = \sum_{i,j=1}^n \mathbf{M}_{ij} v_j = 0, \tag{3.14}$$

and by the definition of the density (1.16), we obtain that

$$\sum_{i=1}^n \int_\Omega \gamma M_i c_i v_i \cdot \tau - \int_\Omega \gamma u \cdot \tau + \int_\Omega \nabla c_{\mathrm{T}} \cdot \tau = 0, \tag{3.15}$$

for all $\tau \in L^2(\Omega)^d$. Considering the first and second terms with the choice $\tau = \nabla w$ for some $w \in H^1_{\Gamma_D}(\Omega)$, and using (3.12),

$$\begin{aligned} \sum_{i=1}^n \int_\Omega \gamma M_i c_i v_i \cdot \nabla w - \int_\Omega \gamma u \cdot \nabla w &= \sum_{i=1}^n \gamma \Big(-\int_\Omega M_i r_i w + \int_{\Gamma_N} M_i g_i w \Big) - \int_\Omega \gamma u \cdot \nabla w \\ &= -\int_\Omega \gamma w \nabla \cdot u + \int_{\Gamma_N} \gamma w u \cdot \mathbf{n} - \int_\Omega \gamma u \cdot \nabla w \quad \text{(by (3.5) and (3.8))} \\ &= 0, \end{aligned} \tag{3.16}$$

the final equality following from integration by parts. In light of this, (3.15) becomes

$$\int_\Omega \nabla c_{\mathrm{T}} \cdot \nabla w = 0, \tag{3.17}$$

for every $w \in H^1_{\Gamma_D}(\Omega)$. In particular, as c_{T} is constant on Γ_D by (3.6), there exists a $w \in H^1_{\Gamma_D}(\Omega)$ such that $\nabla w = \nabla c_{\mathrm{T}}$. For this choice of w, (3.17) becomes

$$\int_\Omega \big| \nabla c_{\mathrm{T}} \big|^2 = 0. \tag{3.18}$$

Hence $\nabla c_{\mathrm{T}} = 0$ almost everywhere, which is the Gibbs–Duhem equation (1.11). The relationship (3.6) ensures that $c_{\mathrm{T}} = C_{\mathrm{T}}$. Equation (3.15) then simplifies to

$$\int_\Omega \Big(\sum_{i=1}^n M_i c_i v_i \Big) \cdot \tau = \int_\Omega u \cdot \tau \quad \forall\ \tau \in L^2(\Omega)^d, \tag{3.19}$$

a variational statement of the mass-flux constraint (1.14).

REMARK 3.2 With pure Neumann boundary data ($\Gamma_D = \emptyset$), the system (3.11)-(3.12) is not well posed. Observe that if c_i and v_i solve equations (3.11) and (3.12) then so do the variables $\hat{c}_i = \alpha c_i$ and $\hat{v}_i = \alpha^{-1} v_i$ for any $\alpha > 0$. In order to make the problem well posed it is necessary to impose auxiliary conditions such as

$$\int_\Omega c_i = \bar{C}_i, \quad i = 1, 2, \ldots, n, \tag{3.20}$$

for known constants $\bar{C}_i$. The physical interpretation of this constraint is clear. In the transient dynamics we have the continuity equations

$$\frac{\partial c_i}{\partial t} = -\nabla \cdot (c_i v_i) + r_i. \tag{3.21}$$

Integrating over Ω and using the divergence theorem we deduce that

$$\frac{d}{dt} \int_\Omega c_i = -\int_\Omega g_i + \int_\Omega r_i. \tag{3.22}$$

For a steady-state solution to exist, it is necessary that the right hand side of this equation is 0. Therefore, for all time t,

$$\frac{d}{dt} \int_\Omega c_i = 0. \tag{3.23}$$

Hence the integral in (3.20) is independent of time and therefore $\bar{C}_i$ is completely specified by the initial conditions.

4. Linearization and well-posedness

We consider a linearization of Picard type. The general approach is that whenever a velocity is multiplied by a concentration, we replace the concentration with our current guess. The exception to this is explained in Remark 4.1. Let us define the function spaces $X = H^1(\Omega)^n$, $X_{\Gamma_D} = H^1_{\Gamma_D}(\Omega)^n$, $Q = (L^2(\Omega)^d)^n$ as well as the affine function space $X_{\tilde{f}} = (H^1_{f_1}(\Omega), \ldots, H^1_{f_n}(\Omega))$. We set the norm on X_{Γ_D} as $\|\cdot\|_{X_{\Gamma_D}} = \|\cdot\|_{H^1_0(\Omega)^n}$. Throughout the rest of this paper we will frequently use the notation $\tilde{q} = (q_1, \ldots, q_n)$ to denote an n-tuple in one of these function/affine function spaces as well as their discrete subspaces.

Given a previous guess for the concentration $\tilde{c}^k = (c_1^k, \ldots, c_n^k)$, we define a bilinear form $a_{\tilde{c}^k}(\cdot,\cdot) : Q \times Q \to \mathbb{R}$ given by

$$a_{\tilde{c}^k}(\tilde{v}, \tilde{\tau}) = \sum_{i=1}^n \int_\Omega \Big(\sum_{j \neq i}^n \frac{c_i^k c_j^k}{\mathscr{D}_{ij} c_{\mathrm{T}}} (v_i - v_j) + \frac{\gamma M_i c_i^k}{\rho^k} \sum_{j=1}^n M_j c_j^k v_j \Big) \cdot \tau_i = \sum_{i,j}^n \int_\Omega \mathbf{M}^{\gamma,k}_{ij} v_j \cdot \tau_i, \tag{4.1}$$

for $\tilde{\tau}, \tilde{v} \in Q$. Here $\mathbf{M}^{\gamma,k}$ denotes the augmented transport matrix, the i,j entries being defined by using the current guess for the concentration $\tilde{c}^k$ in equations (1.8) and (1.18). Similarly, ρ^k is the density evaluated using $\tilde{c}^k$ in (1.16).

For the current guess $\tilde{c}^k$ we also define the bilinear form $b_{\tilde{c}^k} : Q \times X \to \mathbb{R}$,

$$b_{\tilde{c}^k}(\tilde{\tau}, \tilde{w}) = \sum_{i=1}^n \int_\Omega c_i^k \tau_i \cdot \nabla w_i, \tag{4.2}$$

for $(\tilde{\tau}, \tilde{w}) \in Q \times X$, and the bilinear form $b : Q \times X \to \mathbb{R}$,

$$b(\tilde{\tau}, \tilde{w}) = \sum_{i=1}^{n} \int_{\Omega} \tau_i \cdot \nabla w_i. \tag{4.3}$$

For $\tilde{\tau} \in Q$ the linear functional $l_{\tilde{c}^k}(\cdot) : Q \to \mathbb{R}$ is defined as

$$l_{\tilde{c}^k}(\tilde{\tau}) = \gamma \sum_{i=1}^{n} \int_{\Omega} \frac{c_i^k M_i}{\rho^k} \tau_i \cdot u. \tag{4.4}$$

The non-linear iteration scheme is as follows. We take an initial guess $(\tilde{v}^0, \tilde{c}^0) \in Q \times X_{\tilde{f}}$ which satisfies the Dirichlet boundary data (3.3) and

$$\sum_{i=1}^{n} c_i^0 = c_{\mathrm{T}} \tag{4.5}$$

almost everywhere for a given constant c_{T}, determined by either (3.6) or (3.20). For $k = 0, 1, 2, \ldots$ the next iterate of the sequence is computed as the solution to the following generalized saddle point problem: find $(\tilde{v}^{k+1}, \tilde{c}^{k+1}) \in Q \times X_{\tilde{f}}$ such that

$$a_{\tilde{c}^k}(\tilde{v}^{k+1}, \tilde{\tau}) + b(\tilde{\tau}, \tilde{c}^{k+1}) = l_{\tilde{c}^k}(\tilde{\tau}), \ \ \forall\, \tilde{\tau} \in Q, \tag{4.6}$$

$$b_{\tilde{c}^k}(\tilde{v}^{k+1}, \tilde{w}) = -(\tilde{r}, \tilde{w})_{L^2(\Omega)^n} + (\tilde{g}, \tilde{w})_{L^2(\Gamma_N)^n}, \quad \forall\, \tilde{w} \in X_{\Gamma_D}, \tag{4.7}$$

subject to the Dirichlet conditions (3.4). This is repeated until

$$\|\tilde{c}^{k+1} - \tilde{c}^k\|_X + \|\tilde{v}^{k+1} - \tilde{v}^k\|_Q \leqslant \varepsilon, \tag{4.8}$$

for a set tolerance $\varepsilon > 0$.

Note that $(\tilde{v}^k, \tilde{c}^k)$ is a weak solution to the non-linear problem (3.11)-(3.12) if and only if it is a fixed point of this iteration scheme. Indeed if $(\tilde{v}^k, \tilde{c}^k)$ is a weak solution to the non-linear problem (3.11)-(3.12) then the solution $(\tilde{v}^{k+1}, \tilde{c}^{k+1})$ to the equations (4.6)-(4.7) remains $(\tilde{v}^k, \tilde{c}^k)$. Conversely if $(\tilde{v}^{k+1}, \tilde{c}^{k+1}) = (\tilde{v}^k, \tilde{c}^k)$ then, converting (4.6)-(4.7) to a non-linear system by replacing $\tilde{c}^k$ with $\tilde{c}^{k+1}$, we recover the non-linear problem (3.11)-(3.12) and observe it is solved with $(\tilde{v}^{k+1}, \tilde{c}^{k+1})$.

We proceed to prove well-posedness of the linear system (4.6)-(4.7) by applying either Theorem 2.1 in Ciarlet *et al.* (2003) or Theorem 3.1 in Nicolaides (1982). To invoke these theorems we shall prove the following conditions.

Condition 1: There exists a constant $\alpha > 0$ such that

$$a_{\tilde{c}^k}(\tilde{v}, \tilde{v}) \geqslant \alpha \|\tilde{v}\|_Q^2 \tag{4.9}$$

for all $\tilde{v} \in Q$.

Condition 2: There exist constants $\beta_i > 0$, $i = 1, 2$ such that for all $\tilde{w} \in X$,

$$\begin{aligned} \sup_{\tau \in Q} \frac{b(\tilde{\tau}, \tilde{w})}{\|\tilde{\tau}\|_Q} &\geqslant \beta_1 \|\tilde{w}\|_X, \\ \sup_{\tau \in Q} \frac{b_{\tilde{c}^k}(\tilde{\tau}, \tilde{w})}{\|\tilde{\tau}\|_Q} &\geqslant \beta_2 \|\tilde{w}\|_X. \end{aligned} \tag{4.10}$$

REMARK 4.1 An alternative to our definition of the linear functional (4.4) would be to replace $\tilde{c}^k$ with $\tilde{c}^{k+1}$ and therefore include the term as part of the bilinear functional $b(\cdot,\cdot)$ instead. However, the current formulation (4.6)-(4.7) ensures that we can derive the equivalent of (3.15) for the linearized system

$$\sum_{i=1}^{n}\int_{\Omega}\gamma M_i c_i^k v_i\cdot\tau-\int_{\Omega}\gamma u\cdot\tau+\int_{\Omega}\sum_{i=1}^{n}\nabla c_i^{k+1}\cdot\tau=0. \tag{4.11}$$

Then, following an argument identical to that presented in section 3, we deduce that for each k, the iterates satisfy

$$\sum_{i=1}^{n}c_i^{k+1}=c_{\mathrm{T}} \tag{4.12}$$

almost everywhere. When combined with the assumption that the concentrations are positive almost everywhere, this implies that $a_{\tilde{c}^k}(\cdot,\cdot),b(\cdot,\cdot),b_{\tilde{c}^k}(\cdot,\cdot)$ are all bounded bilinear functionals on their respective function spaces.

REMARK 4.2 The common alternative, to formulate the problem in terms of molar fluxes rather than velocities, has the advantage that the continuity equations do not need to be linearized. However, a disadvantage is that the resulting bilinear form $a(\cdot,\cdot)$ is no longer symmetric or coercive, which would add significant difficulty to the analysis.

In order to prove (4.9) it will be useful to write the bilinear form, $a_{\tilde{c}^k}(\cdot,\cdot)$ as the integral of a quadratic form. For this purpose it is useful to define the matrix

$$\mathscr{M}^{\gamma,k}=\mathbf{M}^{\gamma,k}\otimes\mathbf{I} \tag{4.13}$$

where $\mathbf{I}$ is the $d\times d$ identity matrix and $\otimes$ is the Kronecker product. We can then write the bilinear form as

$$a_{\tilde{c}^k}(\tilde{v},\tilde{\tau})=\int_{\Omega}\tilde{\tau}\cdot\mathscr{M}^{\gamma,k}\tilde{v}. \tag{4.14}$$

To show the coercivity condition (4.9) we must show for some $\alpha>0$

$$a_{\tilde{c}^k}(\tilde{v},\tilde{v})=\int_{\Omega}\tilde{v}\cdot\mathscr{M}^{\gamma,k}\tilde{v}\geqslant\int_{\Omega}\alpha|\tilde{v}|^2 \tag{4.15}$$

Hence (4.9) is satisfied if and only if $\mathscr{M}^{\gamma,k}$ is uniformly positive definite over Ω almost everywhere. Either by direct calculation, or by using a standard property of the Kronecker delta product, one can verify that $\mathscr{M}^{\gamma,k}$ will have the same eigenvalues as $\mathbf{M}^{\gamma,k}$, each with geometric multiplicity of d. Therefore coercivity of the bilinear form $a_{\tilde{c}^k}(\cdot,\cdot)$ is equivalent to showing that $\mathbf{M}^{\gamma,k}$ is symmetric positive definite almost everywhere in Ω.

Assuming that every component of our current guess $\tilde{c}^k$ is strictly positive almost everywhere, we prove positive definiteness of $\mathbf{M}^{\gamma,k}$ in the following lemma.

LEMMA 4.1 If $c_i^k\geqslant\kappa>0$ a.e. for each $i=1,2,\ldots,n$ and a positive constant κ, then for any $\gamma>0$, the matrix $\mathbf{M}^{\gamma,k}$ is symmetric positive definite almost everywhere.

Proof. For almost every $x\in\Omega$, $\mathbf{M}^k$ is symmetric positive semidefinite. We proceed with the following argument pointwise. The normalized eigenvectors $\{\vartheta_1^M,\ldots,\vartheta_n^M\}$ form an orthonormal basis. By hypothesis the associated eigenvalues $\{\lambda_1^{\mathbf{M}},\ldots,\lambda_n^{\mathbf{M}}\}$ can be ordered such that

$$0=\lambda_1^{\mathbf{M}}<\lambda_2^{\mathbf{M}}\leqslant\cdots\leqslant\lambda_n^{\mathbf{M}}. \tag{4.16}$$

The nullspace of $\mathbf{M}^k$ then consists of the space spanned by the vector $\vartheta_1^M = n^{-1/2}(1,1,\ldots,1) \in \mathbb{R}^n$. Furthermore,

$$\lambda_2^{\mathbf{M}} \geqslant \lambda_\kappa > 0 \tag{4.17}$$

for a λ_κ that depends only on κ.

Given any $\tilde{\vartheta} \in \mathbb{R}^n$ we can expand it in terms of the basis $\{\vartheta_1^M, \ldots, \vartheta_n^M\}$ as

$$\tilde{\vartheta} = \sum_{i=1}^{n} \alpha_i \vartheta_i^M \tag{4.18}$$

for basis coefficients $\{\alpha_i\}_{i=1}^n$. Furthermore, by orthonormality,

$$\tilde{\vartheta} \cdot \mathbf{M}^k \tilde{\vartheta} = \sum_{i=1}^{n} \lambda_i^{\mathbf{M}} |\alpha_i|^2. \tag{4.19}$$

The matrix $\mathscr{L}^k$ defined in (1.19) is also symmetric positive semidefinite, explicitly for $\tilde{\vartheta} = (\vartheta_1, \ldots, \vartheta_n) \in \mathbb{R}^n$

$$\tilde{\vartheta} \cdot \mathscr{L}^k \tilde{\vartheta} = \frac{1}{\rho^k} \Big(\sum_{j=1}^{n} M_j c_j^k \vartheta_j \Big)^2. \tag{4.20}$$

Hence we can also construct a basis $\{\vartheta_1^{\mathscr{L}}, \ldots, \vartheta_n^{\mathscr{L}}\}$ of orthonormal eigenvectors. The vector ϑ_1^M is also an eigenvector of $\mathscr{L}^k$ with the eigenvalue ρ^k. We will identify this eigenvector as $\vartheta_1^{\mathscr{L}}$. $\mathscr{L}^k$ is of rank 1 as it is the outer product of a vector with itself, and hence all other eigenvalues are zero.

Hence for a given $\tilde{\vartheta} \in \mathbb{R}^n$ we can expand it as

$$\tilde{\vartheta} = \alpha_1 \vartheta_1^M + \sum_{i=2}^{n} \beta_i \vartheta_i^{\mathscr{L}}, \tag{4.21}$$

for basis coefficients $\{\beta\}_{i=1}^n$ and calculate

$$\tilde{\vartheta} \cdot \mathscr{L}^k \tilde{\vartheta} = \rho^k |\alpha_1|^2. \tag{4.22}$$

Consequently,

$$\tilde{\vartheta} \cdot \mathbf{M}^{\gamma,k} \tilde{\vartheta} = \gamma \rho^k |\alpha_1|^2 + \sum_{i=2}^{n} \lambda_i^{\mathbf{M}} |\alpha_i|^2 \tag{4.23}$$

and therefore $\mathbf{M}^{\gamma,k}$ is positive definite at x. This argument can be repeated for every $x \in \Omega$ except perhaps on a set of measure zero. Therefore $\mathbf{M}^{\gamma,k}$ is symmetric positive definite almost everywhere. □

REMARK 4.3 It is useful to understand how λ_κ scales with κ. This can be achieved by the following scaling argument. Suppose that whenever $c_i^k \geqslant 1$ for each $i = 1,2,\ldots,n$ we have the lower bound on the eigenvalues, as in (4.17), of $\lambda_{\kappa=1}$. Now suppose that for any $\kappa > 0$ we have $c_i^k \geqslant \kappa$ for each $i = 1,2,\ldots,n$. We can then define the new variables $\kappa_i = c_i^k/\kappa$. We then see that $\kappa_i \geqslant 1$ for each i. Define the $\mathbf{M}_\kappa$ as the transport matrix with these new variables κ_i replacing c_i. By direct calculation we can check that

$$\mathbf{M}_\kappa = \frac{1}{\kappa} \mathbf{M}. \tag{4.24}$$

By construction we have that $\lambda_2^{\mathbf{M}_\kappa} \geqslant \lambda_{\kappa=1}$. It follows from (4.24) that $\lambda_2^{\mathbf{M}} = \kappa \lambda_2^{\mathbf{M}_\kappa} \geqslant \kappa \lambda_{\kappa=1}$. Hence we see that $\lambda_\kappa = \mathrm{O}(\kappa)$.

LEMMA 4.2 Assume that $\bar{c}_i \geqslant \kappa > 0$ a.e. for each $i = 1,2,\ldots,n$ and $\gamma > 0$. Then the bilinear forms $a(\cdot,\cdot), b(\cdot,\cdot)$ and $b_{\tilde{c}^k}(\cdot,\cdot)$ satisfy the conditions (4.9) and (4.10) for some constants α, β_1, β_2 respectively, which depend only on κ, Ω.

Proof. From Lemma (4.1) we have that

$$a_{\tilde{c}^k}(\tilde{v},\tilde{v}) = \int_\Omega \tilde{\tau}\cdot\mathscr{M}^{\gamma,k}\tilde{v} = \sum_{i,j}\int_\Omega v_j\cdot\mathbf{M}_{ij}^{\gamma,k}v_i \geqslant \alpha\|\tilde{v}\|_Q^2, \tag{4.25}$$

where

$$\alpha = \min\{\gamma\rho^k, \lambda_\kappa\}, \tag{4.26}$$

and λ_κ is as in equation (4.17). This proves condition (4.9).

For conditions (4.10), given a $\tilde{w} \in X$, we can choose $\tilde{\tau} = \nabla\tilde{w}$ which then yields

$$b(\nabla\tilde{w},\tilde{w}) = \sum_{i=1}^n \int_\Omega |\nabla w_i|^2 = \|\tilde{w}\|_{X_{\Gamma_D}}. \tag{4.27}$$

Similarly for $b_{\tilde{c}^k}$ we have

$$b_{\tilde{c}^k}(\nabla\tilde{w},\tilde{w}) \geqslant \kappa\|\tilde{w}\|_{X_{\Gamma_D}}. \tag{4.28}$$

The final step is that we use either $\Gamma_D \neq \emptyset$ or the condition (3.20) to deduce a Poincaré inequality of the form

$$C_p\|\tilde{w}\|_{X_{\Gamma_D}} \geqslant \|\tilde{w}\|_X \text{ for all } \tilde{w} \in X \tag{4.29}$$

for some constant $C_p > 0$ depending only on Ω. Hence

$$b(\nabla\tilde{w},\tilde{w}) \geqslant C_p^{-1}\|\tilde{w}\|_X \tag{4.30}$$

$$b_{\tilde{c}^k}(\nabla\tilde{w},\tilde{w}) \geqslant \kappa C_p^{-1}\|\tilde{w}\|_X. \tag{4.31}$$

□

THEOREM 4.1 Assume $\gamma > 0$ and the current guess $\tilde{c}^k$ satisfies $c_i^k \geqslant \kappa > 0$ a.e. for each $i = 1,2,\ldots,n$ and a positive constant κ. Then, under the condition $\Gamma_D \neq \emptyset$ or (3.20), there exists a unique $(\tilde{v}^{k+1},\tilde{c}^{k+1}) \in Q \times X_{\tilde{f}}$ which solves the system (4.6)-(4.7).

Proof. Our remaining obstacle for the proof is that $X_{\tilde{f}}$ is not a Hilbert space. If we use the ansatz $\tilde{c}^{k+1} = \hat{c}_0^{k+1} + \tilde{c}^0$, where $\hat{c}_0^{k+1} \in X_{\Gamma_D}$ and $\tilde{c}^0 \in X_{\tilde{f}}$ was our initial guess, then we can recast the saddle point problem (4.6)-(4.7) as: find $(\tilde{v}^{k+1},\hat{c}_0^{k+1}) \in Q \times X_{\Gamma_D}$ such that

$$a_{\tilde{c}^k}(\tilde{v}^{k+1},\tilde{\tau}) + b(\tilde{\tau},\hat{c}_0^{k+1}) = l_{\tilde{c}^k}(\tilde{\tau}) - b(\tilde{\tau},\tilde{c}^0) \;\; \forall\,\tilde{\tau} \in Q, \tag{4.32}$$

$$b_{\tilde{c}^k}(\tilde{v}^{k+1},\tilde{w}) = -(\tilde{r},\tilde{w})_{L^2(\Omega)^n} + (\tilde{g},\tilde{w})_{L^2(\Gamma_N)^n} \;\; \forall\,\tilde{w} \in X_{\Gamma_D}. \tag{4.33}$$

By (Ciarlet *et al.*, 2003, Theorem 2.1) or (Nicolaides, 1982, Theorem 3.1) there exists a unique $(\tilde{v}^{k+1},\hat{c}_0^{k+1}) \in Q \times X_{\Gamma_D}$ solution to this system. The proof concludes by observing that if $\tilde{c}^{k+1} = \hat{c}_0^{k+1} + \tilde{c}^0$ then $\tilde{c}^{k+1} \in X_{\tilde{f}}$ and satisfies the system (4.6)-(4.7). □

5. Discretization and error estimates

Here we discretize the generalized saddle point problem (4.6)-(4.7) and prove error estimates. Let $\mathscr{T}_h$ be a regular triangulation of Ω with maximum diameter h. For $m \geqslant 1$ we define the finite dimensional subspaces,

$$Q_h = \{\tilde{\tau}_h \in Q \mid \ \tau_{h,i}\big|_K \in P^{m-1}(K)\ \forall K \in \mathscr{T}_h,\ i = 1,2,\ldots,n\}, \tag{5.1}$$

$$X_h = \{\tilde{w}_h \in X \mid \ w_{h,i}\big|_K \in P^{m}(K)\ \forall K \in \mathscr{T}_h,\ i = 1,2,\ldots,n\}, \tag{5.2}$$

$$X_{\Gamma_D,h} = \{\tilde{w}_h \in X_{\Gamma_D} \mid \ w_{h,i}\big|_K \in P^{m}(K)\ \forall K \in \mathscr{T}_h,\ i = 1,2,\ldots,n\}. \tag{5.3}$$

Here $P^m(K)$ denotes the set of m^{th} order polynomials on the cell $K \in \mathscr{T}_h$.

We will require linear interpolation operators on the spaces X and Q, see (Boffi *et al.*, 2013, pp 72).

PROPOSITION 5.1 There exist linear interpolation operators $\Pi_h : X \to X_h$ and $\Lambda_h : Q \to Q_h$ and constants C_1, C_2 such that, for any $\tilde{c} \in X$, $\tilde{v} \in Q$,

$$\|\tilde{c} - \Pi_h \tilde{c}\|_X \leqslant C_1 h^m \|\tilde{c}\|_{H_0^{m+1}(\Omega)^n},$$
$$\|\tilde{v} - \Lambda_h \tilde{v}\|_Q \leqslant C_2 h^m \|\tilde{v}\|_{(H_0^m(\Omega)^d)^n}.$$

Our non-linear iteration scheme in the discrete case is as follows; we take an initial guess $\tilde{c}^0 \in X_{\tilde{f}}$ which satisfies (4.5) and then construct $\tilde{c}_h^0 := \Pi_h \tilde{c}^0 \in X_h$. The Dirichlet boundary conditions (3.4) are typically only satisfied approximately; however we note that, due to linearity of the interpolation operator and equation (4.5),

$$\sum_{i=1}^{n} c_{i,h}^0 = \sum_{i=1}^{n} \Pi_h c_i^0 = \Pi_h c_{\mathrm{T}} = c_{\mathrm{T}}, \tag{5.4}$$

and therefore condition (3.6) remains enforced.

For $k = 0, 1, 2, \ldots$ the next iterate of the sequence $(\tilde{v}_h^{k+1}, \tilde{c}_h^{k+1})$ is computed by solving the following linear system: find $(\tilde{v}_h^{k+1}, \hat{c}_{0,h}^{k+1}) \in Q_h \times X_{\Gamma_D,h}$ such that

$$a_{\tilde{c}_h^k}(\tilde{v}_h^{k+1}, \tilde{\tau}_h) + b(\tilde{\tau}_h, \hat{c}_{0,h}^{k+1}) = l_{\tilde{c}_h^k}(\tilde{\tau}_h) - b(\tilde{\tau}_h, \tilde{c}_h^0)\ \ \forall\, \tilde{\tau}_h \in Q_h, \tag{5.5}$$

$$b_{\tilde{c}_h^k}(\tilde{v}_h^{k+1}, \tilde{w}_h) = -(\tilde{r}_h, \tilde{w}_h)_{L^2(\Omega)^n} + (\tilde{g}, \tilde{w}_h)_{L^2(\Gamma_N)^n}\ \ \forall\, \tilde{w}_h \in X_{\Gamma_D,h}. \tag{5.6}$$

We then set $\tilde{c}_h^{k+1} = \hat{c}_{0,h}^{k+1} + \tilde{c}_h^0$ and repeat this until $\|\tilde{c}_h^{k+1} - \tilde{c}_h^k\|_X + \|\tilde{v}_h^{k+1} - \tilde{v}_h^k\|_Q \leqslant \varepsilon$ for our tolerance $\varepsilon > 0$.

A distinct advantage of our formulation is that the coercivity condition (4.9) and the inf-sup condition (4.10) are automatically satisfied with the same constants α, β_1, β_2. This follows from the fact that the choice of function spaces preserves a crucial structure:

$$\text{for any } \tilde{w} \in X_h,\ \nabla \tilde{w} \in Q_h, \tag{5.7}$$

which in particular allows us to repeat the proofs of (4.9) and (4.10) in the discrete setting in exactly the same manner. We thus have the following.

THEOREM 5.2 Assume $\gamma > 0$ and that $\tilde{c}_h^k$ satisfies $c_{i,h}^k \geqslant \kappa > 0$ a.e. for each $i = 1, 2, \ldots, n$ and a positive constant κ. Then, under the condition $\Gamma_D \neq \emptyset$ or (3.20), there exists a unique $(\tilde{v}_h^{k+1}, \hat{c}_{0,h}^{k+1}) \in Q_h \times X_{\Gamma_D,h}$ which solves the system (5.5)-(5.6).

Given the well-posedness of the discretized system, we proceed to obtain error estimates. However, given that we have the conditions (4.9)-(4.10) satisfied for the spaces Q_h and X_h, we can use a known result for generalized saddle point systems (Nicolaides, 1982, Theorem 4.1) to deduce the following.

THEOREM 5.3 There exist constants L_1, L_2 depending only on $\alpha, \beta_1, \beta_2, \Omega$ such that

$$\|\hat{c}_0^{k+1} - \hat{c}_{0,h}^{k+1}\|_{X_{\Gamma_D}} \leqslant L_1 \Big(\inf_{\tilde{w}_h \in X_{\Gamma_D,h}} \|\hat{c}_0^{k+1} - \tilde{w}_h\|_X + \inf_{\tilde{\tau}_h \in Q_h} \|\tilde{v}^{k+1} - \tilde{\tau}_h\|_Q \Big), \tag{5.8}$$

$$\|\tilde{v}^{k+1} - \tilde{v}_h^{k+1}\|_Q \leqslant L_2 \Big(\inf_{\tilde{w}_h \in X_{\Gamma_D,h}} \|\hat{c}_0^{k+1} - \tilde{w}_h\|_X + \inf_{\tilde{\tau}_h \in Q_h} \|\tilde{v}^{k+1} - \tilde{\tau}_h\|_Q \Big). \tag{5.9}$$

We have by the Poincaré inequality (4.29) and Proposition 5.1, for some constants C_p, C_1,

$$\|\tilde{c}^{k+1} - \tilde{c}_h^{k+1}\|_X \leqslant \|\hat{c}_0^{k+1} - \hat{c}_{0,h}^{k+1}\|_X + \|\tilde{c}^0 - \tilde{c}_h^0\|_X, \tag{5.10}$$

$$\leqslant C_p^{-1} \|\hat{c}_0^{k+1} - \hat{c}_{0,h}^{k+1}\|_{X_{\Gamma_D}} + C_1 h^m \|\tilde{c}^0\|_{H_0^{m+1}(\Omega)}. \tag{5.11}$$

Therefore, noting that $\Pi_h \hat{c}_0^{k+1} \in X_{\Gamma_D,h}$, we can combine Theorem 5.3 and Proposition 5.1 to deduce the following corollary.

COROLLARY 5.1 There exist constants $\bar{C}_1, \bar{C}_2$ depending only on $\alpha, \beta_1, \beta_2, \Omega$ such that

$$\|\tilde{c}^{k+1} - \tilde{c}_h^{k+1}\|_X \leqslant \bar{C}_1 h^m \Big(\|\tilde{c}^0\|_{H_0^{m+1}(\Omega)^n} + \|\hat{c}_0^{k+1}\|_{H_0^{m+1}(\Omega)^n} + \|\tilde{v}^{k+1}\|_{(H_0^m(\Omega)^d)^n} \Big), \tag{5.12}$$

$$\|\tilde{v}^{k+1} - \tilde{v}_h^{k+1}\|_Q \leqslant \bar{C}_2 h^m \Big(\|\tilde{c}^0\|_{H_0^{m+1}(\Omega)^n} + \|\hat{c}_0^{k+1}\|_{H_0^{m+1}(\Omega)^n} + \|\tilde{v}^{k+1}\|_{(H_0^m(\Omega)^d)^n} \Big). \tag{5.13}$$

For example, if we choose $m = 1$ then we have

$$\|\tilde{v}^{k+1} - \tilde{v}_h^{k+1}\|_Q + \|\tilde{c}^{k+1} - \tilde{c}_h^{k+1}\|_X = \mathrm{O}(h). \tag{5.14}$$

In the next section we will observe that actually $\|\tilde{c}^{k+1} - \tilde{c}_h^{k+1}\|_{L^2(\Omega)^n} = \mathrm{O}(h^{m+1})$. Thus it is likely that one can use duality methods to improve the error estimate in the L^2 norm of $\tilde{c}$.

REMARK 5.1 It can be observed in the proof of (Nicolaides, 1982, Theorem 4.1) that the constants L_1, L_2 appearing in Theorem 5.3 scale as $\mathrm{O}(\alpha^{-1})$. Therefore from (4.26) and the scaling argument in Remark 4.3 we then see that the constants $\bar{C}_1, \bar{C}_2$ will scale as $\mathrm{O}(\kappa^{-1})$.

The Gibbs–Duhem equation is preserved up to machine-precision as can observed by the following argument. Replacing c_T with $c_{\mathrm{T},h}$ we can reproduce the argument of section 3 and derive the equivalent of equation (3.18);

$$\int_\Omega |\nabla c_{\mathrm{T},h}|^2 = 0. \tag{5.15}$$

Combining this with (5.4) we see that $c_{\mathrm{T},h} = C_\mathrm{T}$, where C_T is determined by either (3.6) or (3.20). This calculation does not use any approximation based on the mesh size.

6. Numerical results

Two numerical simulations were implemented with our method. The discretization was implemented using the Firedrake software (Rathgeber *et al.*, 2016) and PETSc (Balay *et al.*, 2019, 1997; Dalcin *et al.*, 2011; Hendrickson & Leland, 1995). The arising linear systems were solved using MUMPS (Amestoy *et al.*, 2001, 2006).

6.1 *Numerical example one: Manufactured solution*

We first consider a test case on $\Omega = [0,1]^2$ for which the solution is analytically known in order to validate the error estimates of section 5.

For $n = 4$ the family of manufactured solutions is constructed as follows. For $j = 1,2$ let $k_j(\cdot) : \Omega \to \mathbb{R}$ be a differentiable function with a strict bound $|k_j| < K_j$ for a positive constant K_j. We set

$$c_1 = k_1 + K_1, \;\; c_2 = -k_1 + K_1,$$
$$c_3 = k_2 + K_2, \;\; c_4 = -k_2 + K_2.$$

We further assume that

$$\mathscr{D}_{13} = \mathscr{D}_{14} = \mathscr{D}_{24} = \mathscr{D}_{23}. \tag{6.1}$$

Then for any given mass-flux $u \in L^2(\Omega)^d$ an exact solution is given when

$$v_1 = -\frac{2}{RT}\Big(\frac{K_1}{\mathscr{D}_{12}} + \frac{K_1}{\mathscr{D}_{13}}\Big)\nabla \ln c_1 + \frac{u}{c_{\mathrm{T}}}, \;\; v_2 = -\frac{c_1}{c_2}v_1 + \frac{u}{c_{\mathrm{T}}},$$
$$v_3 = --\frac{2}{RT}\Big(\frac{K_2}{\mathscr{D}_{34}} + \frac{K_1}{\mathscr{D}_{31}}\Big)\nabla \ln c_3 + \frac{u}{c_{\mathrm{T}}}, \;\; v_4 = -\frac{c_3}{c_4}v_3 + \frac{u}{c_{\mathrm{T}}},$$

and, for $i = 1,2,3,4$,

$$r_i = \operatorname{div}\big(c_i v_i\big). \tag{6.2}$$

We then choose $M_i = 1$ for $i = 1,2,3,4$ so that the mass-flux constraint (1.14) is satisfied.

For this numerical experiment we take $RT = 1$ and

$$k_1(x,y) = \frac{1}{2}\exp(8xy(1-y)(1-x)), \;\; k_2(x,y) = \frac{1}{2}\sin(\pi x)\sin(\pi y); \tag{6.3}$$

we can then take $K_1 = K_2 = 1$. We then have $c_{\mathrm{T}} = 4$. For $i = 1,2,3,4$ we pose the Dirichlet boundary conditions

$$c_i = 1, \;\; \text{on } \partial\Omega, \tag{6.4}$$

and set the mass-flux $u = (0,1)^{\top}$.

The diffusion coefficients are chosen as $\mathscr{D}_{12} = \mathscr{D}_{21} = 2$, $\mathscr{D}_{34} = \mathscr{D}_{43} = 3$ and all other diffusion coefficients set to 1. We take $m = 1$ for the discrete spaces (5.1)-(5.2). For our initial guess we choose $c_i^0 = c_{i,h}^0 = 1$ for $i = 1,2,3,4$. We then proceed with the iteration detailed in section 5 and compute the sequence $(\tilde{v}_h^{k+1}, \tilde{c}_h^{k+1})$ until,

$$\|\tilde{c}_h^{k+1} - \tilde{c}_h^k\|_X + \|\tilde{v}_h^{k+1} - \tilde{v}_h^k\|_Q \leqslant \varepsilon, \tag{6.5}$$

and for this k we set $(\tilde{v}, \tilde{c}) = (\tilde{v}^{k+1}, \tilde{c}^{k+1})$. In this experiment we took $\varepsilon = 10^{-13}$ and $\gamma = 1$. The resulting concentration profile and velocity vector field for species 1 are plotted in Figure 1.

To analyse the rate of convergence we define the three errors

$$E_1 = \Big(\sum_{j=1}^{n} \|c_j - c_{j,h}\|^2_{L^2(\Omega)}\Big)^{\frac{1}{2}}, \tag{6.6}$$

$$E_2 = \Big(\sum_{j=1}^{n} \|\nabla c_j - \nabla c_{j,h}\|^2_{L^2(\Omega)^d}\Big)^{\frac{1}{2}}, \tag{6.7}$$

$$E_3 = \Big(\sum_{j=1}^{n} \|v_j - v_{j,h}\|^2_{L^2(\Omega)^d}\Big)^{\frac{1}{2}}, \tag{6.8}$$

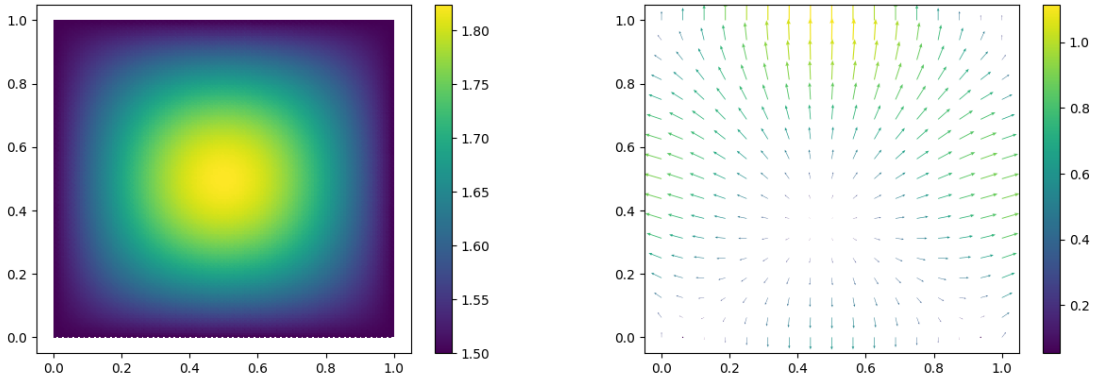

FIG. 1. Concentration of species 1 (left) and its velocity vector field (right). The colour bar on the vector field plot denotes magnitude.

and the error in the mass-flux

$$E_4 = \left\| \sum_{j=1}^{n} M_j c_j v_j - u \right\|_{L^2(\Omega)^d}. \tag{6.9}$$

According to Proposition 5.1, $E_j = \mathrm{O}(h)$ for $i = 1,2,3$. This is validated on the log-log error plot displayed in Figure 2. We also observe that $E_4 = \mathrm{O}(h)$.

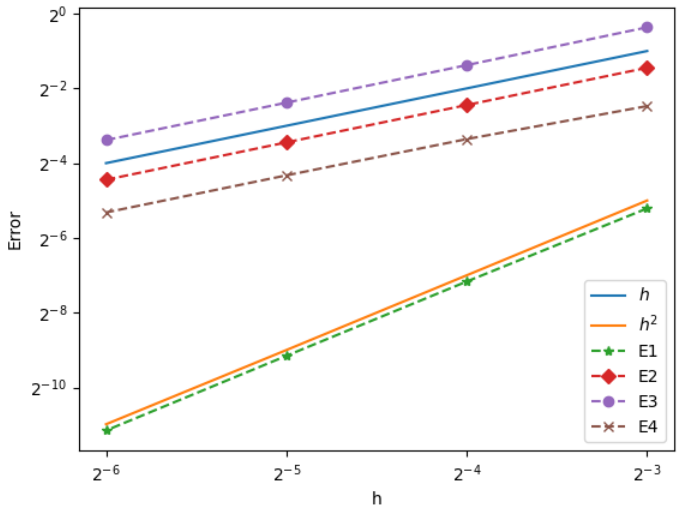

FIG. 2. log-log error plot

Note that we actually observe that $E_1 = \mathrm{O}(h^2)$. This suggests that if one developed a duality-based error

estimate for generalized saddle point systems, the error estimate on E_1 could be improved.

Our discretization also preserves the Gibbs–Duhem relationship up to machine precision, independent of the mesh size. The relevant values are tabulated in Table 1.

Mesh size	Non-linear iterations	$\|\nabla c_{\mathrm{T}}\|_{L^2(\Omega)^d}$
8×8	11	$< 10^{-14}$
16×16	11	$< 10^{-14}$
32×32	11	$< 10^{-14}$
64×64	11	$< 10^{-14}$

TABLE 1. The Gibbs–Duhem relationship is preserved regardless of mesh size

6.2 *Numerical example two: Diffusion of oxygen and effusion of carbon dioxide in the lungs*

If treated as a steady diffusion process, mass transport in the bronchi within the lungs involves simultaneous ingress of oxygen and egress of carbon dioxide. Moreover, the air through which these species diffuse also contains nitrogen and water vapour. For most modelling purposes, it is not necessary to distinguish among the various constituents of air, but in lung modelling we are interested in the distributions of both the oxygen consumed and carbon dioxide produced by the body, as well as the relative humidity along their diffusion paths. The concentrations of these compounds throughout the lungs has been modelled using the Stefan–Maxwell equations in Boudin *et al.* (2010) and Chang *et al.* (1975). For this example we solve for the mole fraction $y_i = c_i/c_{\mathrm{T}}$. Mathematically this is the same as normalising the total concentration to 1. As c_{T} is a constant in this setting, this does not change the weak formulation or the algorithm. We take the mass-flux, u, as zero, and thus consider purely diffusional forces. For a realistic lung model it would be necessary to model the transient dynamics as well as the convective forces and pressure-driven elastic expansion, but this example suffices to illustrate the time-averaged multispecies transport physics.

This simulation was computed on the mesh shown in Figure 3. The surface mesh was provided by C. Geuzaine and J. F. Remacle (Remacle *et al.*, 2010; Marchandise *et al.*, 2011), and from this the 3D mesh was constructed using the software MeshMixer (Schmidt & Singh, 2010) and Gmsh (Geuzaine & Remacle, 2009). The mesh consisted of 115609 vertices and 404174 elements.

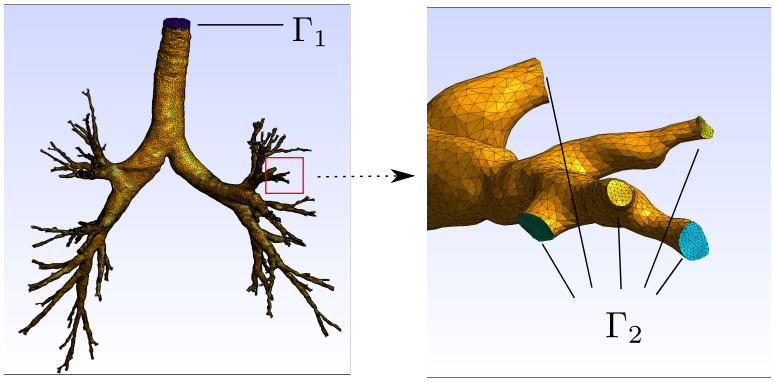

FIG. 3. Mesh of the void space within the lungs at ambient pressure. The surface Γ_1 denotes the inlet at the trachea; the surface Γ_2 is a grouping of all the surfaces at the end of the tertiary bronchi.

Following the two-dimensional numerical experiments performed in Boudin *et al.* (2010), we take mixed Neumann-Dirichlet boundary conditions. At the inlet of the trachea, Γ_1, and at the end of the tertiary bronchi, Γ_2, we set the Dirichlet boundary data to the compositions of humidified air and alveolar air respectively. For the remaining boundary region we set homogeneous Neumann (no-flux) conditions. The Stefan–Maxwell coefficients and the boundary data for this experiment, both taken from Boudin *et al.* (2010), are tabulated in Tables 2 and 3.

TABLE 2. Values of the Stefan–Maxwell diffusion coefficients $\mathscr{D}_{ij}$ between species ($\mathrm{mm}^2\,\mathrm{s}^{-1}$)

Species	N_2	O_2	CO_2	H_2O
N_2		21.87	16.63	23.15
O_2	21.87		16.40	22.85
CO_2	16.63	16.40		16.02
H_2O	23.15	21.87	16.02	

TABLE 3. Dirichlet boundary data at the entrance of the trachea (Γ_1) and the end of the tertiary bronchi (Γ_2). Note that the air is humidified such that the water vapour mole fraction is equal at both Γ_1, Γ_2

	N_2	O_2	CO_2	H_2O
Mole fraction at Γ_1	0.7409	0.1967	0.0004	0.0620
Mole fraction at Γ_2	0.7490	0.1360	0.0530	0.0620

As there are no reactions among the species in the lung, we have $r_i = 0$ for each $i = 1,2,3,4$. The solving parameters were set as $\varepsilon = 10^{-11}$ and $\gamma = 1$. Following our algorithm from section 5, convergence was achieved in 12 non-linear iterations. Each linear system had $5,312,524$ degrees of

freedom and was solved on 12 cores. We remark that despite the very low concentration of carbon dioxide at Γ_1, convergence was achieved in few iterations, and the mole fraction remained positive across all iterations.

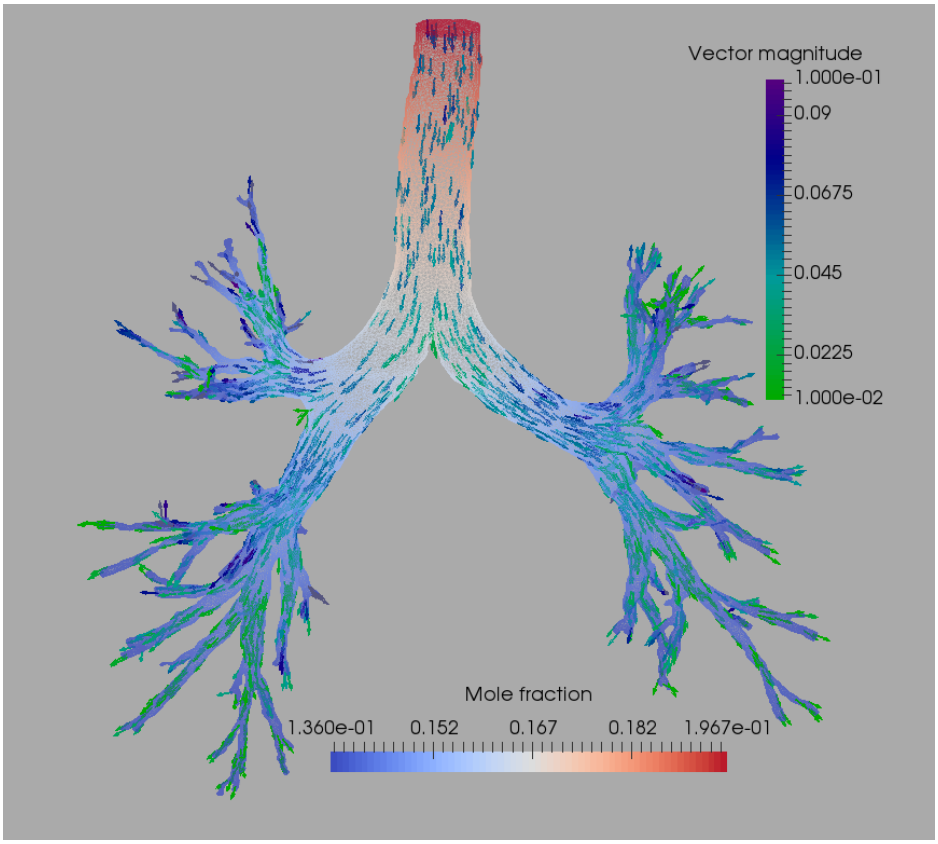

FIG. 4. A plot of the distribution of oxygen in the lungs with its velocity vector field ($\mathrm{mm\,s^{-1}}$).

Interesting physical effects are revealed by the diffusional drag forces in the water vapour. Since the mole fractions for water vapour on the boundaries Γ_1 and Γ_2 are the same, any concentration gradient of water vapour is a consequence of diffusional interactions with the other species.

Figure 5 shows modest uphill diffusion of water vapour at the trachea, where the velocity points in the same direction as the mole-fraction gradient. This can be explained as follows. The difference in the mole fractions of oxygen and carbon dioxide between the trachea and the tertiary bronchi creates a strong mole-fraction gradient, which in turn drives the velocity fields of the respective species in opposing directions. These velocity fields interact with the water vapour and attempt to drag the water vapour along with them, but the diffusional drag force exerted by CO_2 on H_2O exceeds the drag by O_2 on H_2O. Consequently, the water vapour tends to be dragged along with the carbon dioxide — the H_2O velocity flows up the trachea.

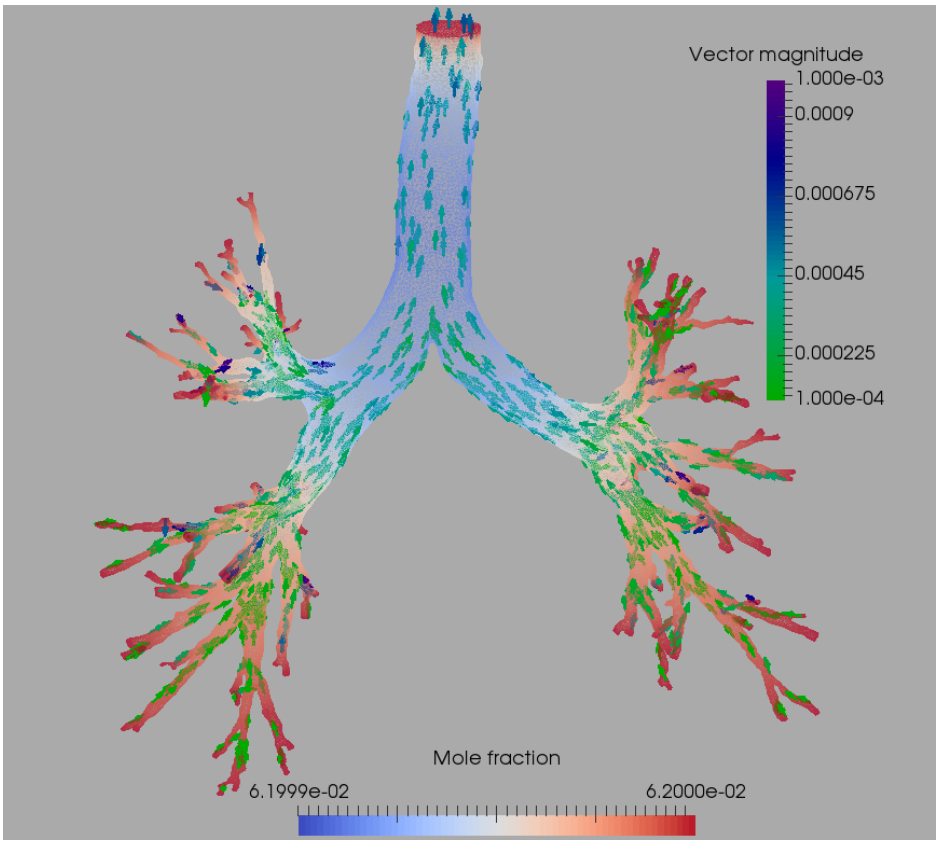

FIG. 5. A plot of the distribution of water vapour in the lungs with its velocity vector field ($\mathrm{mm\,s^{-1}}$).

6.3 *Code availability*

For reproducibility, the exact software versions used to produce the results in this paper, along with instructions for installation, has been archived at `https://zenodo.org/record/3860438`. The exact scripts used to produce each numerical experiment can be found at `https://bitbucket.org/AlexanderVanBrunt/maxwell-stefan-diffusion-equations-repository` along with the mesh used for the lungs.

7. Conclusion

We derived a structure-preserving discretization of the steady-state Stefan–Maxwell diffusion problem based on an augmented saddle point formulation. The inf-sup conditions for the linearized continuous and discrete systems fundamentally rely on the symmetric positive definite structure of an augmented transport matrix, which follows from thermodynamical principles and the construction of the augmentation involving the mass-flux. Error estimates for the general case of n species were then deduced, which were confirmed with numerical experiments.

This work considers idealized assumptions; many real-world applications require the relaxation of these assumptions. Future work will likely involve incorporate solving for momentum and including

more complex driving forces. We hope that the results presented in this paper for the idealized case can provide guiding principles for a more general setting.

8. Acknowledgements

This work was supported by the Engineering and Physical Sciences Research Council Centre for Doctoral Training in Partial Differential Equations: Analysis and Applications (EP/L015811/1), Engineering and Physical Sciences Research Council (EP/R029423/1); the Clarendon fund scholarship; and the Faraday institution SOLBAT project and Multiscale Modelling projects, (subawards FIRG007 and FIRG003 under grant EP/P003532/1). The authors would also like to thank C. Geuzaine and J. F. Remacle for providing the surface of the mesh used in the second numerical example.

REFERENCES

ABDULLAH, N. & DAS, D. (2007) Modelling nutrient transport in hollow fibre membrane bioreactor for growing bone tissue with consideration of multi-component interactions. *Chemical Engineering Science*, **62**, 5821–5839.

AMESTOY, P. R., DUFF, I. S., L'EXCELLENT, J.-Y. & KOSTER, J. (2001) A fully asynchronous multifrontal solver using distributed dynamic scheduling. *SIAM Journal on Matrix Analysis and Applications*, **23**, 15–41.

AMESTOY, P. R., GUERMOUCHE, A., L'EXCELLENT, J.-Y. & PRALET, S. (2006) Hybrid scheduling for the parallel solution of linear systems. *Parallel Computing*, **32**, 136–156.

BAEHR, A. L. & BRUELL, C. J. (1990) Application of the Stefan-Maxwell equations to determine limitations of Fick's law when modeling organic vapor transport in sand columns. *Water Resources Research*, **26**, 1155–1163.

BALAY, S., GROPP, W. D., MCINNES, L. C. & SMITH, B. F. (1997) Efficient management of parallelism in object oriented numerical software libraries. *Modern Software Tools in Scientific Computing* (E. Arge, A. M. Bruaset & H. P. Langtangen eds). Birkhäuser Press, pp. 163–202.

BALAY, S., ABHYANKAR, S., ADAMS, M. F., BROWN, J., BRUNE, P., BUSCHELMAN, K., DALCIN, L., EIJKHOUT, V., GROPP, W. D., KARPEYEV, D., KAUSHIK, D., KNEPLEY, M. G., MAY, D. A., MCINNES, L. C., MILLS, R. T., MUNSON, T., RUPP, K., SANAN, P., SMITH, B. F., ZAMPINI, S., ZHANG, H. & ZHANG, H. (2019) PETSc users manual. *Technical Report* ANL-95/11 - Revision 3.11. Argonne National Laboratory.

BIZERAY, A., HOWEY, D. & MONROE, C. (2016) Resolving a discrepancy in diffusion potentials, with a case study for Li-Ion batteries. *Journal of The Electrochemical Society*, **163**, E223–E229.

BOCHEV, P. B. & LEHOUCQ, R. (2006) Regularization and stabilization of discrete saddle-point variational problems. *Electronic Transactions on Numerical Analysis*, **22**, 97–113.

BOFFI, D., BREZZI, F. & FORTIN, M. (2013) *Mixed Finite Element Methods and Applications*. Springer Series in Computational Mathematics. Berlin Heidelberg: Springer.

BOTHE, D. (2010) On the Maxwell-Stefan approach to multicomponent diffusion. *Progress in Nonlinear Differential Equation and Their Applications*, **80**, 81–93.

BOUDIN, L., GÖTZ, D. & GREC, B. (2010) Diffusion models of multicomponent mixtures in the lung. *ESAIM: Proceedings.*, **30**, 90–103.

BOUDIN, L., GREC, B. & SALVARANI, F. (2012) A mathematical and numerical analysis of the Maxwell-Stefan diffusion equations. *Discrete and Continuous Dynamical Systems - Series B*, **17**, 1427–1440.

BOUSQUET, A., HU, X., METTI, M. & XU, J. (2018) Newton solvers for drift-diffusion and electrokinetic equations. *SIAM Journal on Scientific Computing*, **40**, B982–B1006.

CARTY, R. & SCHRODT, T. (1975) Concentration profiles in ternary gaseous diffusion. *Industrial & Engineering Chemistry Fundamentals*, **14**, 276–278.

CHANG, H.-K., TAI, R. C. & FARHI, L. E. (1975) Some implications of ternary diffusion in the lung. *Respiration Physiology*, **23**, 109–120.

CIARLET, P., HUANG, J. & ZOU, J. (2003) Some observations on generalized saddle-point problems. *SIAM Journal on Matrix Analysis and Applications*, **25**, 224–236.

DALCIN, L. D., PAZ, R. R., KLER, P. A. & COSIMO, A. (2011) Parallel distributed computing using Python. *Advances in Water Resources*, **34**, 1124–1139.

DARKEN, L. S. (1948) Diffusion, mobility and their interrelation through free energy in binary metallic systems. *Transactions of the AIME*, **175**, 184–201.

DATTA, R. & VILEKAR, S. A. (2010) The continuum mechanical theory of multicomponent diffusion in fluid mixtures. *Chemical Engineering Science*, **65**, 5976–5989.

DE GROOT, S. R. & MAZUR, P. (1962) *Non-Equilibrium Thermodynamics*. Amsterdam: North-Holland.

DUNCAN, J. B. & TOOR, H. L. (1962) An experimental study of three component gas diffusion. *AIChE Journal*, **8**, 38–41.

EVANS, L. (2010) *Partial Differential Equations*. Graduate studies in mathematics. Providence, R.I.: American Mathematical Society.

FICK, A. (1855) Über Diffusion. *Annalen der Physik*, **170**, 59–86.

FORTIN, M. & GLOWINSKI, R. (1983) *Augmented Lagrangian Methods: Application to the Solution of Boundary-Value Problems*. Studies in Mathematics and its Applications, vol. 15. Amsterdam-New York, North-Holland: Elsevier.

GEUZAINE, C. & REMACLE, J. F. (2009) Gmsh: A 3-D finite element mesh generator with built-in pre- and post-processing facilities. *International Journal for Numerical Methods in Engineering*, **79**, 1309–1331.

GOYAL, P. & MONROE, C. W. (2017) New foundations of Newman's theory for solid electrolytes: thermodynamics and transient balances. *Journal of The Electrochemical Society*, **164**, E3647–E3660.

HELFAND, E. (1960) On inversion of the linear laws of irreversible thermodynamics. *The Journal of Chemical Physics*, **33**, 319–322.

HENDRICKSON, B. & LELAND, R. (1995) A multilevel algorithm for partitioning graphs. *Supercomputing '95: Proceedings of the 1995 ACM/IEEE Conference on Supercomputing*. New York, NY, USA: Association for Computing Machinery, pp. 28–es.

HERZ, M., RAY, N. & KNABNER, P. (2012) Existence and uniqueness of a global weak solution of a Darcy-Nernst-Planck-Poisson system. *GAMM-Mitteilungen*, **35**, 191–208.

HIRSCHFELDER, J., CURTISS, C. & BIRD, R. (1954) *The Molecular Theory of Gases and Liquids*. New York: John Wiley & Sons.

JÜNGEL, A. & LEINGANG, O. (2019) Convergence of an implicit Euler Galerkin scheme for Poisson-Maxwell-Stefan systems. *Advances in Computational Mathematics*, **45**, 1469–1498.

JÜNGEL, A. & STELZER, I. (2012) Existence analysis of Maxwell-Stefan systems for multicomponent mixtures. *SIAM Journal on Mathematical Analysis*, **45**, 2421–2440.

KOLESNIKOV, A. F. & TIRSKII, G. A. (1984) The Stefan-Maxwell equations for diffusion fluxes of plasma in a magnetic field. *Fluid Dynamics*, **19**, 643–649.

KRAAIJEVELD, G. & WESSELINGH, J. A. (1993) Negative Maxwell–Stefan diffusion coefficients. *Industrial & Engineering Chemistry Research*, **32**, 738–742.

KRISHNA, R. & WESSELINGH, J. (1997) The Maxwell-Stefan approach to mass transfer. *Chemical Engineering Science*, **52**, 861–911.

LIGHTFOOT, E. N., CUSSLER, E. L. & RETTIG, R. L. (1962) Applicability of the Stefan–Maxwell equations to multicomponent diffusion in liquids. *AIChE Journal*, **8**, 708–710.

LIU, C., METTI, M. & XU, J. (2015) Energetically stable discretizations for charge carrier transport and electrokinetic models. *Journal of Computational Physics*, **306**, 1–18.

LIU, J. & MONROE, C. W. (2014) Solute-volume effects in electrolyte transport. *Electrochimica Acta*, **135**, 447–460.

MARCHANDISE, E., CARTON DE WIART, C., VOS, W. G., GEUZAINE, C. & REMACLE, J. (2011) High-quality surface remeshing using harmonic maps—Part II: Surfaces with high genus and of large aspect ratio. *International Journal for Numerical Methods in Engineering*, **86**, 1303–1321.

MAXWELL, J. C. (1867) IV. On the dynamical theory of gases. *Philosophical Transactions of the Royal Society of London*, **157**, 49–88.

MCLEOD, M. & BOURGAULT, Y. (2014) Mixed finite element methods for addressing multi-species diffusion using the Maxwell–Stefan equations. *Computer Methods in Applied Mechanics and Engineering*, **279**, 515–535.

MONROE, C. W., WHEELER, D. R. & NEWMAN, J. (2015) Nonequilibrium linear response theory: application to Onsager–Stefan–Maxwell diffusion. *Industrial & Engineering Chemistry Research*, **54**, 4460–4467.

MONROE, C. W. & DELACOURT, C. (2013) Continuum transport laws for locally non-neutral electrolytes. *Electrochimica Acta*, **114**, 649–657.

MONROE, C. W. & NEWMAN, J. (2009) Onsager's shortcut to proper forces and fluxes. *Chemical Engineering Science*, **64**, 4804–4809.

NERNST, W. (1888) Zur Kinetik der in Lösung befindlichen Körper. *Zeitschrift für Physikalische Chemie*, **2U**, 613–637.

NEWMAN, J., BENNION, D. & TOBIAS, C. W. (1965) Mass transfer in concentrated binary electrolytes. *Berichte der Bunsengesellschaft für physikalische Chemie*, **69**, 608–612.

NEWMAN, J. & THOMAS-ALYEA, K. (2012) *Electrochemical Systems*. Hoboken, New Jersey: John Wiley & Sons.

NICOLAIDES, R. A. (1982) Existence, uniqueness and approximation for generalized saddle point problems. *SIAM Journal on Numerical Analysis*, **19**, 349–357.

ONSAGER, L. (1931a) Reciprocal relations in irreversible processes. I. *Physical Review*, **37**, 405–426.

ONSAGER, L. (1931b) Reciprocal relations in irreversible processes. II. *Physical Review*, **38**, 2265–2279.

ONSAGER, L. (1945) Theories and problems of liquid diffusion. *Annals of the New York Academy of Sciences*, **46**, 241–265.

PLANCK, M. (1890) Über die Potentialdifferenz zwischen zwei verdünnten Lösungen binärer Electrolyte. *Annalen der Physik*, **276**, 561–576.

RATHGEBER, F., HAM, D. A., MITCHELL, L., LANGE, M., LUPORINI, F., MCRAE, A. T. T., BERCEA, G.-T., MARKALL, G. R. & KELLY, P. H. J. (2016) Firedrake: automating the finite element method by composing abstractions. *ACM Transactions on Mathematical Software*, **43**, 24:1–24:27.

REMACLE, J., GEUZAINE, C., COMPÈRE, G. & MARCHANDISE, E. (2010) High-quality surface remeshing using harmonic maps. *International Journal for Numerical Methods in Engineering*, **83**, 403–425.

ROBERTSON, B. C. & ZYDNEY, A. L. (1988) A Stefan-Maxwell analysis of protein transport in porous membranes. *Separation Science and Technology*, **23**, 1799–1811.

SCHMIDT, R. & SINGH, K. (2010) Meshmixer: an interface for rapid mesh composition. *ACM SIGGRAPH 2010 Talks*. Association for Computing Machinery.

SCHMUCK, M. (2009) Analysis of the Navier–Stokes–Nernst–Planck–Poisson System. *Mathematical Models and Methods in Applied Sciences*, **19**.

STANDART, G. L., TAYLOR, R. & KRISHNA, R. (1979) The Maxwell-Stefan formulation of irreversible thermodynamics for simultaneous heat and mass transfer. *Chemical Engineering Communications*, **3**, 277–289.

STEFAN, J. (1871) Über das Gleichgewicht und die Bewegung, insbesondere die Diffusion von Gasgemengen. *Sitzungsberichte der Mathematisch-Naturwissenschaftlichen Classe der Kaiserlichen Akademie der Wissenschaften Wien, 2te Abteilung*, **63**, 63–124.

VILLALUENGA, I., PESKO, D. M., TIMACHOVA, K., FENG, Z., NEWMAN, J., SRINIVASAN, V. & BALSARA, N. P. (2018) Negative Stefan–Maxwell diffusion coefficients and complete electrochemical transport characterization of homopolymer and block copolymer electrolytes. *Journal of The Electrochemical Society*, **165**, A2766–A2773.